

Final Draft
of the original manuscript:

Li, Z.; Wang, W.; Kratz, K.; Kuechler, J.; Xu, X.; Zou, J.; Deng, Z.; Sun, X.;
Gossen, M.; Ma, N.; Lendlein, A.:

**Influence of surface roughness on neural differentiation of human
induced pluripotent stem cells**

In: Clinical Hemorheology and Microcirculation (2016) IOS Press

DOI: 10.3233/CH-168121

Influence of surface roughness on neural differentiation of human induced pluripotent stem cells

Zhengdong Li ^{1,2}, Weiwei Wang ¹, Karl Kratz ^{1,3}, Judit K uchler ^{1,#}, Xun Xu ^{1,2}, Jie Zou ^{1,2}, Zijun Deng ¹, Xianlei Sun ¹, Manfred Gossen ^{1,3}, Nan Ma ^{1,2,3,*} and Andreas Lendlein ^{1,2,3,*}

¹Institute of Biomaterial Science and Berlin-Brandenburg Center for Regenerative Therapies, Helmholtz-Zentrum Geesthacht, Kantstra e 55, 14513 Teltow, Germany

²Institute of Chemistry and Biochemistry, Freie Universit t Berlin, Takustra e 3, 14195 Berlin, Germany

³Helmholtz Virtual Institute - Multifunctional Materials in Medicine, Berlin and Teltow, Kantstra e 55, 14513 Teltow, Germany

* To whom correspondence should be addressed:

Prof. Dr. Nan Ma, Prof. Dr. Andreas Lendlein

Email: nan.ma@hzg.de, andreas.lendlein@hzg.de

Phone: +49 (0)3328 352-450

Fax: +49 (0)3328 352-452

#Present address: Berlin Institute of Health, Stem Cell Core Facility, Augustenburger Platz 1, 13353 Berlin, Germany

Abstract

Induced pluripotent stem cells (iPSCs) own the capacity to develop into all cell types of the adult body, presenting high potential in regenerative medicine. Regulating and controlling the differentiation of iPSCs using the surface topographic cues of biomaterials is a promising and safe approach to enhance their therapeutic efficacy. In this study, we tested the effects of surface roughness on differentiation of human iPSCs into neural progenitor cells and dopaminergic neuron cells using polystyrene with different roughness (R0: flat surface; R1: rough surface, $R_q \sim 6 \mu\text{m}$; R2: rough surface, $R_q \sim 38 \mu\text{m}$). Neural differentiation of human iPSCs could be influenced by surface roughness. Up-regulated neuronal markers were found in cells on rough surface, as examined by real-time PCR and immunostaining. Particularly, the R1 surface significantly improved the neuronal marker expression, as compared to R0 and R2 surface. This study

demonstrates the significance of surface roughness, depending on the roughness level, in promoting differentiation of human iPSCs towards the neuronal lineage. Our study suggests the potential applications of surface roughness in iPSCs based treatment of neural disorder diseases, and highlights the importance of design and development of biomaterials with effective surface structures to regulate stem cells.

Key words: human iPSCs, roughness, neural differentiation, regenerative medicine

1 Introduction

Induced pluripotent stem cells (iPSCs), generated from adult cells by introducing transcription factors, hold great promise in regenerative medicine without many of the associated ethical concerns as compared to embryonic stem cells (ESC) [1,36]. Due to their neural differentiation capacity, iPSCs have been described as scientific breakthrough for treating Parkinson's Disease (PD), which is a common neurodegenerative disorder characterized by a selective loss of dopaminergic neurons. In this area, remarkable progress has been made in the past decade. For example, the dopaminergic neurons as the predominant cell type for treating PD have been effectively generated from iPSCs [17,30], and functionally integrated into cynomolgus monkey model [14]. These achievements presage a strong immunological, functional and biological rationale to use dopamine neurons derived from iPSCs for cell replacement in PD in the future. However, there are still some challenges that need to be overcome such as inefficient cell derivation or genetic abnormalities during *in vitro* expanding [29]. Most of all, it is of utmost importance to avoid the teratoma or tumor formation caused by inadequate differentiation [15]. It is only of benefit if there is a complete differentiation to generate the cell types of interest. Hence, controlled neural differentiation of iPSCs is critical for treating PD by cell replacement.

Researchers have assembled considerable knowledge on how biochemical factors, signaling pathways and transcriptional networks regulate iPSCs behaviors [11]. Increasing evidences have demonstrated that the biophysical properties of the microenvironment, such as the extracellular matrix (ECM) stiffness and cyclic strain, could effectively control a variety of cell behaviors of iPSCs [5,6]. Most of the biophysical properties can be readily generated using the appropriate fabrication technologies, such as the topographic features at micro- and nano-scale which have shown effects to induce changes in cell alignment, polarization, elongation, migration,

proliferation and gene expression [13,20,23]. It has been reported recently that the topography of nano- and micro-grating substrates could regulate the expression of neuronal markers in iPSCs [25]. Further, appropriate microscale roughness could affect the differentiation of mesenchymal stem cells [12]. Therefore, topographical cues might hold a great interest in inducing neural dopaminergic differentiation of iPSCs.

In this study, we hypothesized that surface roughness could influence the neural differentiation of human iPSCs. To examine our hypothesis, neural differentiation was induced in a polystyrene-based cell culture insert system with different roughness on the bottom. Considering the single cell size of human iPSCs ($\sim 43.5 \mu\text{m}^2$) [32], surfaces with three different roughness levels were used (R0: flat surface; R1: rough surface, $R_q \sim 6 \mu\text{m}$; R2: rough surface, $R_q \sim 38 \mu\text{m}$) to adapt the cell size. Human iPSCs were induced to differentiate into neural progenitor cells and dopaminergic cells on matrigel-coated inserts. The expression of neural ectodermal marker genes and neural marker proteins was assessed. Our results indicated that the differentiation of human iPSCs was promoted by the microscale roughness. Cells on R1 presented the highest level of neural differentiation. These results expand the knowledge of improving neural differentiation of iPSCs by topographic cues, which would be a benefit for design and fabrication of biomaterials to enhance efficacy of iPSCs-based regenerative therapies.

2 Materials and methods

2.1 Cell culture surfaces

Polystyrene (PS) inserts fitting the standard 24-well tissue culture plate (TCP) were prepared via injection molding as described before [28,33]. Three differently structured cylinders were utilized to manufacture the inserts with different types of bottom roughness: a cylinder with a polished contact surface (R0), and two cylinders with micro-structured surfaces according to the standard of German Institute for Standardization (DIN 16747: 1981-05), M30 (R1) and M45 (R2). The prepared inserts were sterilized by gas sterilization (gas phase: 10% ethylene oxide, 54 °C, 65% relative humidity, 1.7 bar, 3 hours of gas exposure time and 21 hours of aeration phase). The roughness of the insert bottom was determined with an optical profilometer (MicoProf 200, FRT

- Fries Research & Technologie GmbH, Bergisch Gladbach, Germany) equipped with a CWL 300 chromatic white-light sensor. The data were acquired with the software AQUIRE (ver. 1.21) and were evaluated with the software MARK III (ver. 3.9).

The PS inserts and tissue culture plate were coated with MatrigelTM Basement Membrane Matrix (BD Biosciences; San Jose, USA) to enable the cell attachment. Matrigel was diluted with Dulbecco's Modified Eagle Medium-Nutrient Mixture F-12 (DMEM/F12, Thermo Fisher Scientific, Bonn, Germany) (1:80 v/v). For each well of 6 well TCP or each PS insert, 2000 μ l or 200 μ l (approximately 200 μ l/cm²) of diluted matrigel solution was added and incubated at 37 °C for 1 h, and then was removed before cell cultivation.

2.2 Human iPSCs cultivation and neural differentiation

Human iPSCs (IMR90-4 cell line, WiCell, Wisconsin, USA) were cultured in feeder-free medium (mTeSRTM, STEMCELL Technologies, Vancouver, Canada) on matrigel-coated dishes at 37 °C in a humidified atmosphere containing 5% CO₂. For cell maintenance, the medium was changed regularly and the cells were passaged every 5 days at ratios of 1:6.

The neuronal differentiation conditions were adapted from Dual SMAD inhibition protocol [2]. Briefly, the iPSCs clusters were dissociated into single cells with cell detachment solution (AccutaseTM, STEMCELL Technologies, Vancouver, Canada). Then, the cells were seeded on matrigel-coated dishes or PS inserts at a density of 3×10^4 cells/cm². Neural differentiation was induced at day 4 by changing the culture medium to N2B27 medium (Neurobasal[®] medium (Thermo Fisher Scientific, Bonn, Germany) supplemented with 0.5 mM L-Glutamine (Thermo Fisher Scientific, Bonn, Germany), B-27[®] Supplement (Thermo Fisher Scientific, Bonn, Germany) and N-2[®] Supplement (Thermo Fisher Scientific, Bonn, Germany)) containing different compounds (Fig. 3A). From day 4, N2B27 medium containing 10 μ M SB431542 (Merck Millipore, Darmstadt, Germany Germany), 200 ng/mL Noggin (R&D Systems, Minneapolis, USA) and Dorsomorphin (Sigma-Aldrich, St Louis, USA) was used. At day 8, the medium was replaced with that containing 200 ng/mL recombinant N-terminal human sonic hedgehog (SHH, R&D Systems, Minneapolis, USA) instead of SB431542. From day 12 the induction medium was changed to N2B27 medium supplemented with 20 ng/mL brain-derived neurotrophic factor (BDNF, Peprotech, Hamburg, Deutschland), 100 ng/mL FGF8 (R&D Systems, Minneapolis, USA), 200

μ M ascorbic acid (AA, Sigma-Aldrich, St Louis, USA) and 200 ng/mL SHH. From day 16, N2B27 medium supplemented with 20 ng/mL BDNF, 200 μ M ascorbic acid and 20 ng/mL glial cell-derived neurotrophic factor (GDNF, ProSpec-Tany TechnoGene, Rehovot, Israel) was applied. The medium was changed every 2 days during the whole induction process.

2.3 Immunocytochemistry

The human iPSCs cultured in TCP or PS inserts were fixed by adding 4% paraformaldehyde (Sigma-Aldrich, St. Louis, MO, USA) for 15 minutes and then permeabilized with 0.1% Triton X-100 (Sigma-Aldrich, St. Louis, MO, USA) for 5 minutes. After blocking with 3% bovine serum albumin (BSA) (Sigma-Aldrich, St. Louis, MO, USA) solution for 30 minutes, the cells were incubated with mouse anti-human primary antibodies (mouse monoclonal anti-neuronal β - III Tubulin, mouse monoclonal anti-Nestin and mouse monoclonal anti-MAP2 (all are from Millipore, Darmstadt, Germany)) at 4 °C overnight. After washing with PBS, the secondary antibodies (Alexa Fluor-488 goat anti-mouse IgG, 1:500; Alexa Fluor-555 goat anti-mouse IgG, 1:500; Life Technologies, Darmstadt, Germany) were added and incubated for 60 minutes. The cell nuclei were stained with 4',6-diamidino-2-phenylindole (DAPI, Sigma-Aldrich, St. Louis, MO, USA). After 3 times of washing with PBS, the samples were visualized using a fluorescence microscope (AxioSkop, Carl Zeiss, Jena, Germany) or scanned with a confocal laser scanning microscope (LSM 780, Carl Zeiss, Jena, Germany).

For the cell characterization staining, the human iPSCs were stained with the Fluorescent Human ES/iPS Cell Characterization Kit (Millipore, Darmstadt, Germany) following the manufacturer's protocol.

2.4 Real-time PCR

Isolation of total RNA was performed using TRI Reagent® (Sigma-Aldrich, St. Louis, MO, USA) following the manufacturer's instruction. The cDNA was synthesized from the isolated RNA using Superscript™ III First-Strand Synthesis System (Life Technologies, Darmstadt, Germany) according to the given protocol. Quantitative RT-PCR was performed on a StepOnePlus™ Real-time PCR Systems (Life Technologies, Darmstadt, Germany) using SYBER® Green Master Mix (Thermo Fisher Scientific, Bonn, Germany) and RT-PCR primers (Table 1). The expression of the

genes of interest was determined in triplicate for each cell sample. Glyceraldehyde 3-phosphate dehydrogenase (GAPDH) was used as housekeeping gene. Gene expression level was determined using the method as we described before [34]. The ΔC_T values of the target genes was normalized with the C_T value of GAPDH ($\Delta C_T = C_T, \text{ target} - C_T, \text{ GAPDH}$). The fold change of gene expression levels between two samples was expressed as $2^{-\Delta\Delta C_T}$ ($\Delta\Delta C_T = \Delta C_T, \text{ sample 2} - \Delta C_T, \text{ sample 1}$).

Table 1. Primer sequence

Gene	Primer (Forward)	Primer (Reverse)
<i>GAPDH</i>	GTGGACCTGACCTGCCGTCT	GGAGGAGTGGGTGTCGCTGT
<i>SOX1</i>	AATTTTATTTTCGGCGTTGC	TGGGCTCTGTCTCTTAAATTTGT
<i>SOX2</i>	CCCAGCAGACTTCACATGT	CCTCCCATTTCCCTCGTTTT
<i>NESTIN</i>	CTGGAGCAGGAGAAACAGG	TGGGAGCAAAGATCCAAGAC
<i>PAX6</i>	ATGTGTGAGTAAAATTCTGGGCA	GCTTACAACCTTCTGGAGTCGCTA
<i>MAP2</i>	GGAGACAGAGATGAGAATTCCT	GAATTGGCTCTGACCTGGT

2.5 Western blotting

To quantify the neuronal protein expression, cell lysates were prepared with RIPA buffer (Sigma-Aldrich, St. Louis, MO, USA) supplemented with phenylmethylsulfonyl fluoride (Life Technologies, Darmstadt, Germany) and Protease Inhibitor Cocktails (Sigma-Aldrich, St. Louis, MO, USA). The obtained protein solutions were denatured by heating at 95 °C for 5 minutes, separated by electrophoresis on 10% gradient SDS-poly acrylamide gel and then transferred onto PVDF membranes (Millipore, Darmstadt, Germany). The blots were probed with monoclonal primary antibodies and fluorescently labeled secondary antibodies (Li-Cor, Bad Homburg, Germany). Fluorescent signal were then detected using an Odyssey Imaging scanner and the intensity was analyzed by image studio software (Li-Cor, Bad Homburg, Germany).

2.6 Statistics

Data are shown as mean \pm standard deviation. Statistical analysis was performed using the two-tailed independent-samples t-test, and a significant level (Sig.) < 0.05 was considered to be statistically significant.

3 Results

3.1 Cell culture surfaces characterization

PS inserts with different types of bottom roughness were prepared via injection molding (Fig. 1A-C). The micro-scale roughness of the insert bottom was first determined via optical profilometry measurement. R0 has a smooth surface with the root mean squared roughness (R_q) value around $0.3 \mu\text{m}$, while R1 and R2 have the rougher surfaces with R_q values around $6 \mu\text{m}$ and $38 \mu\text{m}$, respectively. At nanoscale, all of the surfaces are relatively smooth with an average R_q values less than 200 nm (Table 2). The surfaces were coated with matrigel prior to cell seeding. The ECM gel-coated surfaces for human iPSCs seeding were in R_q analysis in the level of uncoated surfaces (Fig. 1 D, Table. 2).

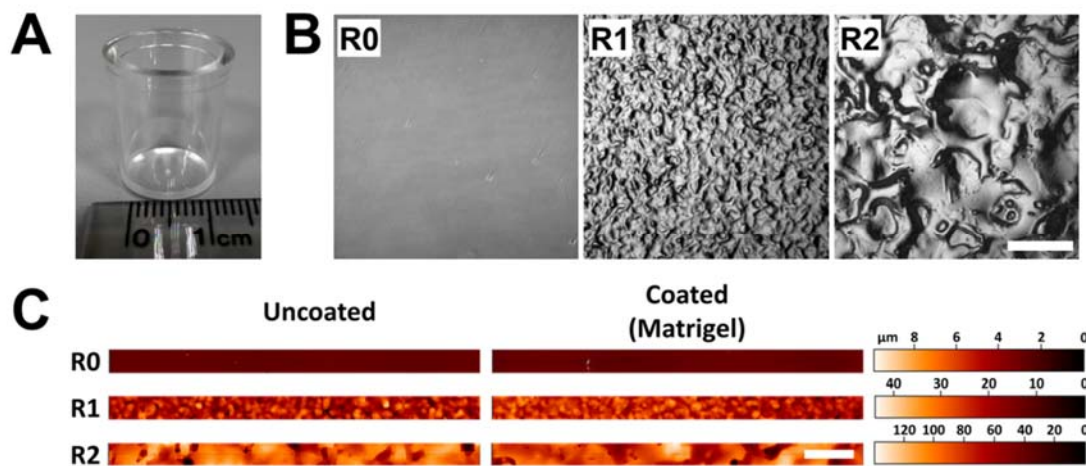


Fig. 1. PS inserts bottom surface characterization. (A) Insert with a suitable size to fit the standard 24-well tissue culture plate. (B) Phase contrast microscope images showed the three types of insert bottom with different roughness (bar = $500 \mu\text{m}$). (C) Representative profilometry scanning images of the surfaces before and after matrigel coating (bar = $500 \mu\text{m}$).

Table 2. Surface roughness

Samples	Uncoated		Matrigel coated
	Micro-roughness ^{a)}	Nano-roughness ^{b)}	Nano-roughness ^{b)}
	R_q (μm)	R_q (μm)	R_q (μm)
R0	0.31 ± 0.11	0.020 ± 0.010	0.015 ± 0.004
R1	6.01 ± 0.21	0.154 ± 0.044	0.138 ± 0.040
R2	38.15 ± 5.86	0.067 ± 0.021	0.093 ± 0.004

^{a)} Optical profilometry measurement by scanning an area of $7 \times 7 \text{ mm}^2$. ^{b)} Optical profilometry measurement by scanning an area of $50 \times 50 \mu\text{m}^2$.

3.2 Human iPSCs characterization

To characterize the human iPSCs, alkaline phosphatase (AP) and pluripotency markers (Oct4 and Nanog) were assessed through immunostaining (Fig. 2). The cultivated human iPSCs showed the typical iPSC colony morphology and a well-defined edge composed of tightly packed cells with round shape and uniform size. The undifferentiated iPSCs positively expressed AP and the iPSC markers Oct4 and Nanog.

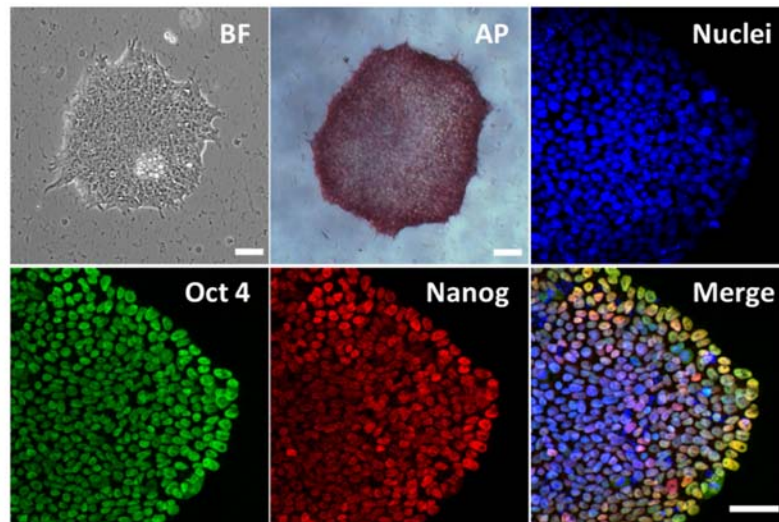


Fig. 2. Human iPSCs characterization. Cultivated iPSCs showed the classic colony morphology and expressed the pluripotency markers of Oct4 and Nanog (bar = $50 \mu\text{m}$).

3.3 Neural differentiation on TCP

At first, the neural differentiation of cultivated human iPSCs was performed on the TCP coated with matrigel. Following the dual SMAD pathway inhibition protocol (Fig. 3, A), the iPSCs were rapidly differentiated into neural progenitor cells which were characterized by immunostaining of Nestin at day 16. The neural progenitor cells derived from iPSCs showed the typical rosette morphology (Fig. 3, B upper panel). During this period, the expression of pluripotency gene Oct 4 was downregulated, and the neural progenitor marker genes PAX6, SOX 1 and Nestin were upregulated (Fig. 3, C). With the further induction with BDNF and GDNF, the neural progenitor cells continuously differentiated into neuronal cells. After 42 days of induction, the cells differentiated from iPSCs expressed the mature neural marker β -III Tublin (Fig. 3, B lower panel).

3.4 Neural differentiation on rough surfaces

To study the influence of topographic roughness on neural differentiation of human iPSCs, the neural induction was performed in the PS inserts with different bottom roughness using the same protocol as that on TCP surface (Fig. 3, A). After 42 days of induction, the cells differentiated from human iPSCs showed the neural microtubule structures and positively expressed the neural identifiable proteins MAP2 and β -III Tublin (Fig. 4).

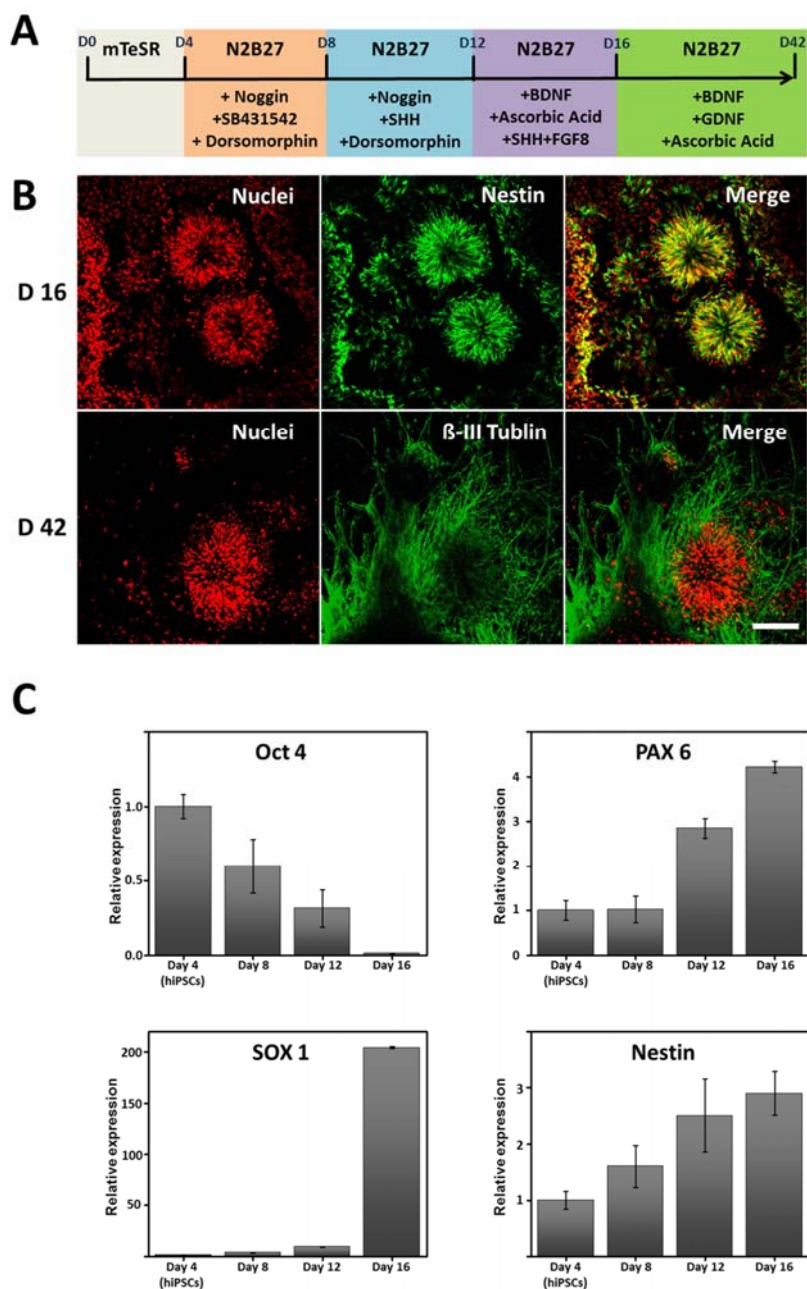


Fig. 3. Human iPSCs neural differentiation on TCP coated with matrigel. (A) The neural differentiation protocol induced by small molecules and growth factors. (B) Representative images of differentiated iPSCs showing identifiable rosette morphology of neural progenitor cells at day 16 (upper panel) and positively expressing the neural marker β -III Tubulin at day 42 (lower panel, bar = 50 μ m). (C) Pluripotency gene (Oct 4) expression was downregulated while neural genes (PAX 6, SOX 1, Nestin) expression were upregulated during induction process. The undifferentiated human iPSCs were used as control (n = 3).

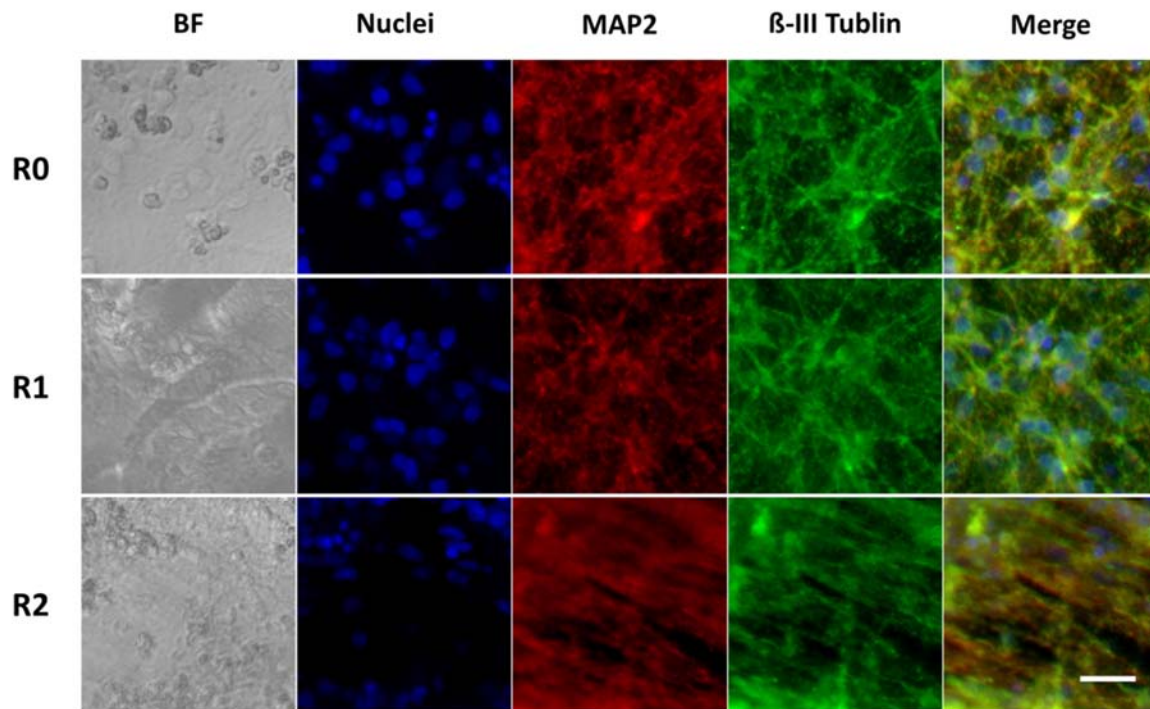


Fig. 4. Neural differentiation of human iPSCs on matrigel-coated surfaces with different roughness. After 42 days of induction, human iPSCs differentiated into neural cells on all surfaces, expressing the neural identification marker β -III Tublin and MAP2 (bar = 25 μ m).

3.5 Neural gene and protein expression

To investigate the effects of roughness on neural differentiation of iPSCs, quantitative real-time PCR was performed to assess the expression of neural genes of the differentiated iPSCs at day 16. Compared with cells on flat surface R0, the neural progenitor cells on rougher surface R1 and R2 exhibited higher expression levels of Nestin and β -III Tublin. Particularly, these genes expressed significantly higher on R1 surface as compared to those on R0 and R2 (Fig. 5, A).

To further investigate the effects of microroughness on neural differentiation, the progenitor cells derived from the human iPSCs were continuously induced into differentiation towards dopaminergic neurons with BDNF, GDNF and AA. After 42 days, the protein expression was assessed by western blot (Fig. 5, B). The cells on R1 surface expressed higher neural proteins

compared with the cells on R0 and R2 surfaces. Notably, cells on R1 expressed significantly higher β - III Tublin than cells on R0 and R2 (Fig. 5, C).

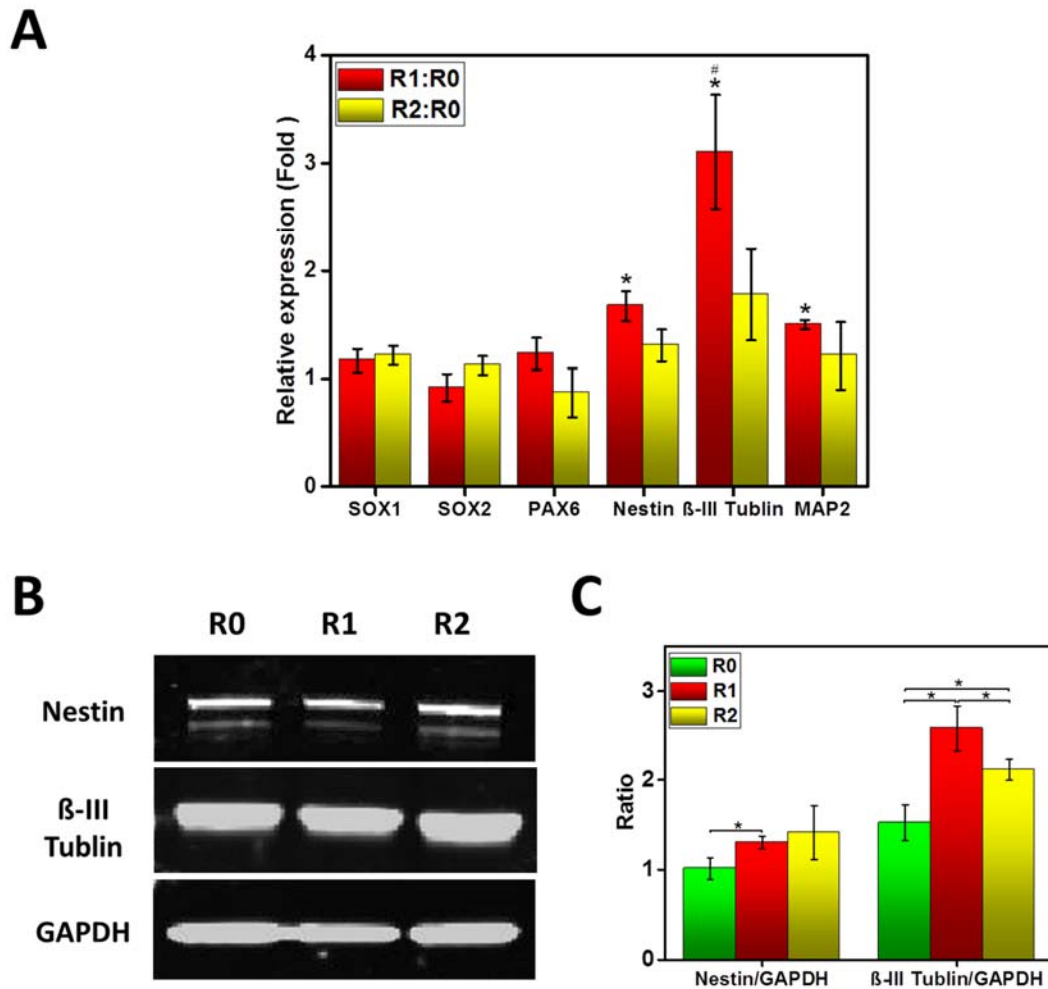


Fig. 5. Expression of neural genes and proteins of iPSCs induced towards neural differentiation on surfaces with different microroughness. (A) After 16 days of induction, the expression of SOX1, SOX2, PAX6, Nestin, β - III Tublin and MAP2 genes was quantified via RT-PCR and normalized to the expression level on R0 surface (n = 3, * R1: R0 Sig. < 0.05, # R1: R2 Sig. < 0.05). (B) After 42 days of induction, the expression of Nestin and β - III Tublin proteins of the cells were analyzed via western blotting. (C) The statistical analysis of Nestin expression and β - III Tublin expression (normalized to GAPDH, n = 3, * Sig. < 0.05).

4 Discussion

Neural differentiation of iPSCs represents a promise in neural regenerative medicine. Due to the tumorigenic potential [7], establishment of efficient neural differentiation approach is an essential prerequisite for further applications. Mechanic cues are increasingly studied to affect stem cell behaviors. Thus, modulation of neural differentiation of iPSCs with different physical cues is of great interest in regenerative medicine. In our work, designed polymer surface systems with different roughness demonstrated that appropriate roughness could promote the dopaminergic neural differentiation of iPSCs in gene and protein expression. Our finding highlights a new approach to enhance the efficiency of dopaminergic neuron derivation of iPSCs.

In the current study, highest promotive effects of differentiation were found on the middle-ranged R1 surface, which might best accommodate to the iPSCs size. It has been reported that nanoscale roughness surfaces tended to induce pluripotent stem cells (PSCs) into spontaneous differentiation while smooth surfaces supported PSCs adhesion, rapid cell proliferation and long-term self-renewal [3]. In our system, higher nanoscale roughness of our designed surfaces was found on R1 and R2 surfaces compared with flat R0 surface. Thus, the elevated neural differentiation on R1 and R2 surface may be attributed not only to the microscale roughness, but also to the nanoscale roughness. This finding indicated an optimal roughness condition for the human iPSCs neural differentiation. However, more deep studies are needed to explore the concealed mechanism.

Several approaches can be considered for the induction of iPSCs neural differentiation. Like the early protocol, embryoid bodies generated from the lifting PSCs, are grown in adherent culture condition in N2 and fibroblast growth factor (bFGF) supplemented medium to form neural progenitor cells which are allowed to form the neural rosettes structure [38]. This embryoid body formation pathway is considered as a distinguishing feature of successful neural differentiation induction. Another approach is to use the mouse stromal feeder cells that are known to have the neural inducing effect [10]. However, the embryoid body formation or feeder cell approaches are not appropriate to study the influence of the roughness on neural differentiation because of the rare direct contact conditions. Recently, a remarkable and robust approach via dual inhibition of SMAD signaling was reported for the neural induction of PSCs [2]. Single cell adherent cultivation of PSCs were stimulated with Noggin (an inhibitor of bone morphogenetic protein 4, BMP4) and

SB431542 (an inhibitor of Lefty/Activin/TGF β pathways) to achieve neural differentiation. For the feasibility and robustness as well as high efficiency, this approach has resulted in its relative popularity in the neural differentiation induction. In this study, Dorsomorphin (a chemical BMP inhibitor) was added to increase the efficiency and reduce the costs [19]. Additionally, the extracellular matrix has great effects on the efficiency of neural differentiation of PSCs [22,24]. Matrigel was chosen to coat the surface in current work due to its great enhancement of neural differentiation [24].

For the source of the human iPSCs, IMR90-4 was chosen in our study. This cell line was generated from IMR90 fetal lung fibroblasts by viral transduction of a combination of Oct 4, Sox 2, Nanog, and Lin 28 genes. In our cultivation, the cells showed the typical iPSCs colony morphology and a well-defined edge composed of tightly packed and uniformly sized cells, and an elevated level of AP on the cell membrane. AP is commonly used to identify the undifferentiated PSCs including ESCs and iPSCs [27,31]. Additionally, the pluripotency markers Oct 4 and Nanog were characterized in our immunostaining. Further, these cells had a high efficiency of differentiation capacity towards neural lineage in a comparative study [16].

In PSCs differentiation, the pluripotency genes and the stage specific lineage genes are downregulated and upregulated respectively. It is reported that Pax6 gene plays a critical role in neural differentiation and determines the human neuroectoderm cell fate [37]. During PSCs differentiation to neural cells, Oct4 is downregulated before Pax6 becomes highly expressed [26]. Our results showed that the Oct4 gene was sustainably downregulated by induction, and the Pax6 gene was conversely upregulated, which is in accordance with these reports. Besides, the neural marker genes Sox1 and Nestin were upregulated during the induction, which is in accordance with previous findings [10].

Our results indicated that the neural gene expression of neural progenitor cells was upregulated after 16 days of induction, and among these genes, the Nestin, β -III Tubulin and MAP2 were significantly upregulated by rough surface R1 compared with the flat surface R0 and although rougher surface R2. This indicated that the roughness promoted neural differentiation, and this promotion was dependent on the roughness level. MAP2 as a mature neuron marker was also upregulated on the rough surface, which demonstrated that roughness could enhance the neuron

maturation from the progenitor stage. Both, Nestin and β -III Tubulin expression were upregulated after dopaminergic neural induction by the R1 rough surface, which revealed that appropriate roughness could increase the neural differentiation of iPSCs. Although the obvious enhancement of neural differentiation was observed, the mechanism of roughness-induced differentiation remains unclear. It may be attributed to the surface roughness-related subtle force, which may cause a difference in membrane attachment and in cellular responses to the guidance signals evoked from the substrates [21], the formation and alignment of focal adhesion kinase (FAK) phosphorylation-involved focal adhesions induced by the topography, which could lead to stem cell differentiation [4,35]. Further, the cytoskeleton rearrangement and nuclei relocation by the roughness may play a critical role in the mechanical signal transduction to affect gene expression [8,9]. In addition, local curvature formed by surface roughness may affect the stem cell differentiation [18].

5 Conclusion

In this work, we demonstrated the roughness effects on human iPSCs differentiation towards neuronal lineage. Neural differentiation of human iPSCs was successfully induced on the matrigel-coated polymeric inserts providing a specific micro and nano roughness. Gene expression profiling by real-time PCR and immunostaining showed significant upregulation of neuronal marker expression on rough surfaces. Notably, middle-ranged rough surface induced the highest level of neuronal marker expression. This study demonstrates the significance of microscale roughness in differentiation of human iPSCs towards neuronal lineage. It suggested the potential application of polymeric surfaces with designed surface roughness in clinical regenerative medicine.

Acknowledgements

The authors acknowledge Mr. Robert Jeziorski and Mr. Mario Rettschlag for preparation of sterilized PS inserts, Dr. Harald Stachelscheid for providing cells, Ms. Katrin Michel for technical support. This work was financially supported by the Helmholtz Association of German Research Centers (programme-oriented funding, as well as Helmholtz-Portfolio Topic “Technology and Medicine”) and the German Federal Ministry of Education and Research (BMBF project number

0315696A “Poly4Bio BB”). The authors comply with the Ethical Guidelines for Publication in Clinical Hemorheology and Microcirculation as published in Clin Hemorheol Microcirc, 63, 2016, 1–2.

References

- [1] J. Bilic and J.C.I. Belmonte, Concise Review: Induced Pluripotent Stem Cells Versus Embryonic Stem Cells: Close Enough or Yet Too Far Apart?, *Stem Cells* **30** (2012), 33-41.
- [2] S.M. Chambers, C.A. Fasano, E.P. Papapetrou, M. Tomishima, M. Sadelain and L. Studer, Highly efficient neural conversion of human ES and iPS cells by dual inhibition of SMAD signaling, *Nat Biotechnol* **27** (2009), 275-80.
- [3] W. Chen, L.G. Villa-Diaz, Y. Sun, S. Weng, J.K. Kim, R.H. Lam, L. Han, R. Fan, P.H. Krebsbach and J. Fu, Nanotopography influences adhesion, spreading, and self-renewal of human embryonic stem cells, *ACS Nano* **6** (2012), 4094-103.
- [4] Y.C. Chen, D.C. Lee, T.Y. Tsai, C.Y. Hsiao, J.W. Liu, C.Y. Kao, H.K. Lin, H.C. Chen, T.J. Palathinkal, W.F. Pong, N.H. Tai, I.N. Lin and I.M. Chiu, Induction and regulation of differentiation in neural stem cells on ultra-nanocrystalline diamond films, *Biomaterials* **31** (2010), 5575-87.
- [5] F. Chowdhury, Y. Li, Y.C. Poh, T. Yokohama-Tamaki, N. Wang and T.S. Tanaka, Soft substrates promote homogeneous self-renewal of embryonic stem cells via downregulating cell-matrix tractions, *PLoS One* **5** (2010), e15655.
- [6] F. Chowdhury, S. Na, D. Li, Y.C. Poh, T.S. Tanaka, F. Wang and N. Wang, Material properties of the cell dictate stress-induced spreading and differentiation in embryonic stem cells, *Nat Mater* **9** (2010), 82-8.
- [7] J.J. Cunningham, T.M. Ulbright, M.F. Pera and L.H. Looijenga, Lessons from human teratomas to guide development of safe stem cell therapies, *Nat Biotechnol* **30** (2012), 849-57.
- [8] M.J. Dalby, M.J. Biggs, N. Gadegaard, G. Kalna, C.D. Wilkinson and A.S. Curtis, Nanotopographical stimulation of mechanotransduction and changes in interphase centromere positioning, *J Cell Biochem* **100** (2007), 326-38.
- [9] M.J. Dalby, N. Gadegaard, P. Herzyk, D. Sutherland, H. Agheli, C.D. Wilkinson and A.S. Curtis, Nanomechanotransduction and interphase nuclear organization influence on genomic control, *J Cell Biochem* **102** (2007), 1234-44.
- [10] Y. Elkabetz, G. Panagiotakos, G. Al Shamy, N.D. Socci, V. Tabar and L. Studer, Human ES cell-derived neural rosettes reveal a functionally distinct early neural stem cell stage, *Genes Dev* **22** (2008), 152-65.
- [11] A.J. Engler, S. Sen, H.L. Sweeney and D.E. Discher, Matrix elasticity directs stem cell lineage specification, *Cell* **126** (2006), 677-89.
- [12] A.B. Faia-Torres, S. Guimond-Lischer, M. Rottmar, M. Charnley, T. Goren, K. Maniura-Weber, N.D. Spencer, R.L. Reis, M. Textor and N.M. Neves, Differential regulation of osteogenic differentiation of stem cells on surface roughness gradients, *Biomaterials* **35** (2014), 9023-32.

- [13] R.G. Flemming, C.J. Murphy, G.A. Abrams, S.L. Goodman and P.F. Nealey, Effects of synthetic micro- and nano-structured surfaces on cell behavior, *Biomaterials* **20** (1999), 573-88.
- [14] P.J. Hallett, M. Deleidi, A. Astradsson, G.A. Smith, O. Cooper, T.M. Osborn, M. Sundberg, M.A. Moore, E. Perez-Torres, A.L. Brownell, J.M. Schumacher, R.D. Spealman and O. Isacson, Successful function of autologous iPSC-derived dopamine neurons following transplantation in a non-human primate model of Parkinson's disease, *Cell Stem Cell* **16** (2015), 269-74.
- [15] S.G. Hong, T. Winkler, C.F. Wu, V. Guo, S. Pittaluga, A. Nicolae, R.E. Donahue, M.E. Metzger, S.D. Price, N. Uchida, S.A. Kuznetsov, T. Kilts, L. Li, P.G. Robey and C.E. Dunbar, Path to the Clinic: Assessment of iPSC-Based Cell Therapies In Vivo in a Nonhuman Primate Model, *Cell Reports* **7** (2014), 1298-1309.
- [16] B.Y. Hu, J.P. Weick, J. Yu, L.X. Ma, X.Q. Zhang, J.A. Thomson and S.C. Zhang, Neural differentiation of human induced pluripotent stem cells follows developmental principles but with variable potency, *Proc Natl Acad Sci U S A* **107** (2010), 4335-40.
- [17] H. Jiang, Y. Ren, E.Y. Yuen, P. Zhong, M. Ghaedi, Z. Hu, G. Azabdaftari, K. Nakaso, Z. Yan and J. Feng, Parkin controls dopamine utilization in human midbrain dopaminergic neurons derived from induced pluripotent stem cells, *Nat Commun* **3** (2012), 668.
- [18] K.A. Kilian, B. Bugarija, B.T. Lahn and M. Mrksich, Geometric cues for directing the differentiation of mesenchymal stem cells, *Proc Natl Acad Sci U S A* **107** (2010), 4872-7.
- [19] D.S. Kim, J.S. Lee, J.W. Leem, Y.J. Huh, J.Y. Kim, H.S. Kim, I.H. Park, G.Q. Daley, D.Y. Hwang and D.W. Kim, Robust Enhancement of Neural Differentiation from Human ES and iPS Cells Regardless of their Innate Difference in Differentiation Propensity, *Stem Cell Reviews and Reports* **6** (2010), 270-281.
- [20] H.J. Kong and D.J. Mooney, Microenvironmental regulation of biomacromolecular therapies, *Nat Rev Drug Discov* **6** (2007), 455-63.
- [21] S. Lenhert, A. Sesma, M. Hirtz, L. Chi, H. Fuchs, H.P. Wiesmann, A.E. Osbourn and B.M. Moerschbacher, Capillary-induced contact guidance, *Langmuir* **23** (2007), 10216-23.
- [22] Y. Li, M. Liu, Y. Yan and S.T. Yang, Neural differentiation from pluripotent stem cells: The role of natural and synthetic extracellular matrix, *World J Stem Cells* **6** (2014), 11-23.
- [23] J.Y. Lim and H.J. Donahue, Cell sensing and response to micro- and nanostructured surfaces produced by chemical and topographic patterning, *Tissue Eng* **13** (2007), 1879-91.
- [24] W. Ma, T. Tavakoli, E. Derby, Y. Serebryakova, M.S. Rao and M.P. Mattson, Cell-extracellular matrix interactions regulate neural differentiation of human embryonic stem cells, *BMC Dev Biol* **8** (2008), 90.
- [25] F. Pan, M. Zhang, G. Wu, Y. Lai, B. Greber, H.R. Scholer and L. Chi, Topographic effect on human induced pluripotent stem cells differentiation towards neuronal lineage, *Biomaterials* **34** (2013), 8131-9.
- [26] M.T. Pankratz, X.J. Li, T.M. Lavaute, E.A. Lyons, X. Chen and S.C. Zhang, Directed neural differentiation of human embryonic stem cells via an obligated primitive anterior stage, *Stem Cells* **25** (2007), 1511-20.
- [27] M.F. Pera, B. Reubinoff and A. Trounson, Human embryonic stem cells, *J Cell Sci* **113** (Pt 1) (2000), 5-10.

- [28] T. Roch, A. Kruger, K. Kratz, N. Ma, F. Jung and A. Lendlein, Immunological evaluation of polystyrene and poly(ether imide) cell culture inserts with different roughness, *Clinical Hemorheology and Microcirculation* **52** (2012), 375-389.
- [29] K. Saha and R. Jaenisch, Technical Challenges in Using Human Induced Pluripotent Stem Cells to Model Disease, *Cell Stem Cell* **5** (2009), 584-595.
- [30] A. Swistowski, J. Peng, Q. Liu, P. Mali, M.S. Rao, L. Cheng and X. Zeng, Efficient generation of functional dopaminergic neurons from human induced pluripotent stem cells under defined conditions, *Stem Cells* **28** (2010), 1893-904.
- [31] K. Takahashi, K. Tanabe, M. Ohnuki, M. Narita, T. Ichisaka, K. Tomoda and S. Yamanaka, Induction of pluripotent stem cells from adult human fibroblasts by defined factors, *Cell* **131** (2007), 861-72.
- [32] S. Wakao, M. Kitada, Y. Kuroda, F. Ogura, T. Murakami, A. Niwa and M. Dezawa, Morphologic and gene expression criteria for identifying human induced pluripotent stem cells, *PLoS One* **7** (2012), e48677.
- [33] W.W. Wang, N. Ma, K. Kratz, X. Xu, Z.D. Li, T. Roch, K. Bieback, F. Jung and A. Lendlein, The influence of polymer scaffolds on cellular behaviour of bone marrow derived human mesenchymal stem cells, *Clinical Hemorheology and Microcirculation* **52** (2012), 357-373.
- [34] X. Xu, W. Wang, K. Kratz, L. Fang, Z. Li, A. Kurtz, N. Ma and A. Lendlein, Controlling major cellular processes of human mesenchymal stem cells using microwell structures, *Adv Healthc Mater* **3** (2014), 1991-2003.
- [35] K. Yang, K. Jung, E. Ko, J. Kim, K.I. Park, J. Kim and S.W. Cho, Nanotopographical manipulation of focal adhesion formation for enhanced differentiation of human neural stem cells, *ACS Appl Mater Interfaces* **5** (2013), 10529-40.
- [36] J. Yu, M.A. Vodyanik, K. Smuga-Otto, J. Antosiewicz-Bourget, J.L. Frane, S. Tian, J. Nie, G.A. Jonsdottir, V. Ruotti, R. Stewart, Slukvin, II and J.A. Thomson, Induced pluripotent stem cell lines derived from human somatic cells, *Science* **318** (2007), 1917-20.
- [37] X.Q. Zhang, C.T. Huang, J. Chen, M.T. Pankratz, J.J. Xi, J. Li, Y. Yang, T.M. LaVaute, X.J. Li, M. Ayala, G.I. Bondarenko, Z.W. Du, Y. Jin, T.G. Golos and S.C. Zhang, Pax6 Is a Human Neuroectoderm Cell Fate Determinant, *Cell Stem Cell* **7** (2010), 90-100.
- [38] Y. Zhang, C. Pak, Y. Han, H. Ahlenius, Z. Zhang, S. Chanda, S. Marro, C. Patzke, C. Acuna, J. Covy, W. Xu, N. Yang, T. Danko, L. Chen, M. Wernig and T.C. Sudhof, Rapid single-step induction of functional neurons from human pluripotent stem cells, *Neuron* **78** (2013), 785-98.